Research Square

Preprints are preliminary reports that have not undergone peer review.
They should not be considered conclusive, used to inform clinical practice,
or referenced by the media as validated information.

Temperature–brucellosis associations in China, 2005–2020: limited evidence for modification by rural depopulation

Fei Wang
First Affiliated Hospital of Xi'an Jiaotong University
Yajuan He
First Affiliated Hospital of Xi'an Jiaotong University
Yuanyuan Duan
Xian Center for Disease Control and Prevention
Mi Ke
First Affiliated Hospital of Xi'an Jiaotong University
Yuxin Liu
First Affiliated Hospital of Xi'an Jiaotong University
Tianyan Chen
First Affiliated Hospital of Xi'an Jiaotong University
Zhen Tian
tianzhen@xjtufh.edu.cn

First Affiliated Hospital of Xi'an Jiaotong University

Article

Keywords: Brucellosis, Rural depopulation, Temperature, Effect modification, Distributed lag non-linear models, China

Posted Date: November 23rd, 2026

DOI: https://doi.org/10.21203/rs.3.rs-11565242/v1

License: This work is licensed under a Creative Commons Attribution 4.0 International License.
Read Full License

Additional Declarations: No competing interests reported.

Temperature–brucellosis associations in China, 2005–2020: limited evidence for modification by rural depopulation

Fei Wang[1,4†], Yajuan He[1,4†], Yuanyuan Duan[3], Mi Ke[1], Yuxin Liu[1], Tianyan Chen[2,4*] & Zhen Tian[1,2,*]

1 Department of Ultrasound, The First Affiliated Hospital of Xi'an Jiaotong University

2 Department of Infectious Diseases, The First Affiliated Hospital of Xi'an Jiaotong University

3 Department of Viral Disease Laboratory, Xi'an Center for Disease Control and Prevention

4 Public Health Center, The First Affiliated Hospital of Xi'an Jiaotong University

† Fei Wang and Yajuan He contributed equally to this work.

* Correspondence: Zhen Tian (tianzhen@xjtufh.edu.cn; ORCID 0000-0001-7475-9472) and Tianyan Chen (chentianyan@xjtufh.edu.cn; ORCID 0000-0002-0721-5739).

Abstract

Climate–disease associations are often assumed to remain stable as exposed populations change. We linked 604,783 notified human brucellosis cases from 31 Chinese provinces (2005–2020) to 0.25° climate data and fitted livestock-adjusted, age-stratified distributed-lag non-linear models. At 27.8 °C versus 14.2 °C, cumulative relative risks were 7.05 (95% confidence interval 3.43–14.50) for ages 0–19 years (16 provinces; sparse paediatric counts), 3.18 (2.15–4.70) for ages 20–59 years, and 2.70 (1.60–4.58) for ages ≥60 years. Warming explained 1.8–3.0% of the model-estimated temperature-attributable burden in the primary analysis, although attributable fractions and warming shares depended on the minimum-risk-temperature search range. In 20 provinces with estimates in both periods, the relative risk at 27 °C for ages 20–59 years was 1.10 (0.60–2.03) in 2005–2012 and 2.37 (0.98–5.73) in 2013–2020. The change-on-change association with rural-share decline was attenuated (slope −0.26; p = 0.075), and single-stage sensitivity models did not corroborate its direction. Temperature–brucellosis associations persisted after livestock adjustment, but evidence for modification by rural depopulation was limited and model-dependent. These findings support climate-sensitive prevention while cautioning against causal interpretation of ecological changes.

Keywords: Brucellosis; Rural depopulation; Temperature; Effect modification; Distributed lag non-linear models; China

Introduction

Whether a climate–disease relationship is stable over time is usually assumed rather than tested. Human brucellosis, a zoonosis acquired through contact with infected livestock and their products, remains a major global health concern, with a conservative estimate of 2.1 million new cases annually and substantial underdiagnosis [1]. China has experienced a marked resurgence since the mid-2000s: after near-elimination in the 1990s, notified human cases climbed steeply through the 2000s and 2010s, concentrated in the northern pastoral belt and among occupationally exposed adults [2]. Livestock intensification, growth of the mutton and dairy markets, and the southward spread of transmission from traditional pastoral regions have all been implicated [2,3].

Two further transformations have run in parallel. The first is climatic: mean temperatures over China rose by roughly half a degree per decade over the same window, lengthening the thermally suitable period for pathogen survival in the environment and reshaping the seasonality of outdoor animal contact. Short-term climate–brucellosis associations are well documented — provincial studies have linked warmer and wetter months to elevated case

counts [3] — but these studies model the temperature relationship as stationary, and none asks whether the relationship itself has changed as the rural social structure that mediates exposure has been transformed. Recent multi-sector research has likewise shown that climatic, environmental and socioeconomic factors jointly shape zoonotic risk [4]. However, identifying risk drivers is not equivalent to testing whether the exposure–response relationship itself changes over time.

The second transformation is demographic. Over the same 16 years, China's rural population share fell from roughly 57% to 36%, driven by massive out-migration of working-age adults. This "rural hollowing-out" changes who handles livestock: plausibly devolving herding, slaughter, and home-processing tasks onto older residual workers, whose heat-stress physiology, protective-behaviour capacity, and baseline exposure patterns differ from those of the departed younger workforce. If temperature acts on transmission through exposure-mediated pathways — outdoor handling peaks in warm months, animal parturition, reduced protective behaviour under heat stress — then the temperature sensitivity of brucellosis should strengthen as the exposed population restructures, independently of how much the climate itself has warmed.

We therefore assembled a nationwide ecological panel of all 604,783 notified human brucellosis cases in China from 2005 to 2020, at the resolution of province × month × single-year age, linked to 0.25° gridded climate observations and province-year socioeconomic covariates, and asked three questions. (RQ1) What is the shape and strength of the temperature–morbidity relationship by age band? (RQ2) How much of the long-term case burden is attributable to non-optimal temperature, and how much of that is specifically due to the observed warming trend — as opposed to background climatic suitability? (RQ3) Does the temperature–morbidity relationship vary with the socioeconomic context of exposure — between provinces, or within provinces over time as rural hollowing-out proceeds? We hypothesised (H1) a monotonic warm-temperature association strongest in the working-age exposed population; (H2) that the warming trend would explain only a small share of the attributable burden, with age-specific (socioeconomic) rate change dominating the long-term trend; and (H3) that temperature sensitivity would emerge over time in provinces undergoing rapid rural depopulation — detectable only in a within-province, change-on-change design, since between-province contrasts conflate climate with livestock structure.

Results

Burden, ageing, and seasonality of cases

Between 2005 and 2020, 604,783 human brucellosis cases were reported across the 31 provincial-level divisions of mainland China. The crude national rate rose from 1.432 to 3.351 per 100,000, peaking in 2014 (4.201 per 100,000) before a partial decline and renewed increase after 2017 (Fig. 1; Table 1). Burden remained heavily concentrated in the northern pastoral belt: the three highest-incidence provincial-level divisions were Inner Mongolia (45.4 per 100,000), Ningxia (17.1) and Xinjiang (14.2) (Table 1). Kitagawa decomposition attributes the national increase (+1.919 per 100,000) overwhelmingly to rising age-specific rates (+1.850) rather than population ageing (+0.069; 3.6% of the change) (Table 2, Panel B).

The age structure of cases shifted markedly towards older adults: the proportion of cases aged ≥60 years rose from 6.7% in 2005 to 22.2% in 2020 (Fig. 2), and age-band-specific trends show incidence rising fastest in the oldest band (APC ≥60 +10.8% per year, 95% CI 7.3 to 14.5), even as the working-age band remained the dominant share of the absolute burden. Seasonality peaked in May, with 38.3% of annual cases concentrated in April–June (Supplementary Fig. S3).

Temperature–morbidity exposure–response relationships

Livestock-adjusted two-stage distributed lag non-linear models (province-specific negative-binomial first stage; random-effects multivariate meta-analytic second stage; cumulative lag 0–2 months; reference = median temperature) yielded a low-to-moderate-heterogeneity pooled exposure–response surface (I^2 0–16%; Fig. 3). The cumulative relative risk increased monotonically with monthly mean temperature in all age bands. At 27.8 °C (95th percentile) versus the 14.2 °C reference, RR was 7.05 (95% CI 3.43–14.50) in ages 0–19, 3.18 (2.15–4.70) in ages 20–59, and 2.70 (1.60–4.58) in ages ≥60 (16, 30, and 25 provinces, respectively). Estimates at 29.2 °C (99th percentile) were 8.64 (3.89–19.21), 3.59 (2.32–5.57) and 3.01 (1.67–5.44), respectively, and are treated as sensitivity estimates. Corresponding original-model RRs at 27.8 °C were 7.14, 2.99 and 2.47; the old and new curves were similar (Supplementary Fig. S4). H1 was not supported by the age pattern of the point estimates, which was steepest in ages 0–19 rather than the working-age band. Because the 0–19 analysis was based on only 16 provinces and sparse paediatric counts, age-specific contact patterns were not measured, and no formal between-age contrast was performed, this finding neither establishes an age difference nor implies greater individual susceptibility.

Climatic attribution and the minor role of warming

The pooled MRT was −8.3 °C in all three age bands, at the lower boundary of the 5th–95th percentile search range. Repeating the attribution with livestock-adjusted pooled curves, the model-estimated AF for non-MRT temperatures was 66.96% in ages 0–19, 48.93% in ages 20–59 and 51.51% in ages ≥60 (Table 2, Panel A). These values are attributable fractions, not observed proportions of cases in months above the MRT. The 2005–2020 warming trend itself (median +0.62 °C per decade across provinces) explained only a small fraction of this attributable burden: warming-associated excess cases were +302, +7,100 and +1,369 for ages 0–19, 20–59 and ≥60, respectively — 1.8–3.0% of climate-attributable cases (Table 2, Panel A). When the MRT search began at the 1st percentile, the MRT shifted to −15.649 °C in all bands; AF increased to 85.90%, 71.52% and 67.70%, while warming-associated excess cases were +128, +3,959 and +912 and warming shares were 0.60%, 1.16% and 1.35%, respectively (Supplementary Table S4). Thus, both AF and the estimated warming contribution depended materially on the reference/search-range definition. Climate sets the stage, but the sixteen-year rise and fall of notified incidence is overwhelmingly a non-climatic story.

Socioeconomic effect modification: between-province and temporal contrasts

Between-province comparisons remained null after livestock adjustment: neither stratified pooling at the median of province-mean rural population share nor meta-regression of province-specific log-RR on rural share showed significant modification (all $p \geq 0.43$; Fig. 4). These analyses do not establish the absence of effect modification.

Exploratory meta-regression suggested stronger temperature–brucellosis associations in provinces with higher livestock-to-rural-population ratios among adults aged 20–59 years. However, these estimates were sensitive to baseline-climate adjustment, mutual livestock adjustment, and weighting, and no corresponding evidence was observed in the other age bands. Livestock-density modification therefore remains exploratory and model-dependent (Supplementary Table S7 and Supplementary Fig. S6).

In common-province, livestock-adjusted period analyses, later-period point estimates were higher but statistically uncertain. In ages 20–59 (20 provinces in both periods), pooled cumulative RR at 27 °C was 1.10 (95% CI 0.60–2.03) in 2005–2012 and 2.37 (0.98–5.73) in 2013–2020 (I^2 = 0% and 11%). In ages ≥60 (14 common provinces), corresponding estimates were 0.64 (0.27–1.54) and 2.56 (0.90–7.29). The early inverse point estimate in older adults was imprecise and compatible with no association; it should not be read as a protective temperature effect. Change-on-change meta-regression was attenuated: slope −0.262 log-RR at 25 °C per percentage-point change in rural share ($p = 0.075$) for ages 20–59 and −0.091 ($p = 0.679$) for ages ≥60 (Table 2, Panel C). Results at 20 °C were likewise non-significant ($p = 0.110$ and 0.716), and ages 0–19 (11 common provinces) showed no

corresponding rural-change association (p = 0.917 at 25 °C). In the same 20 provinces for ages 20–59, fixed-effect weighting without livestock gave a slope of −0.408 (p = 0.009); adding livestock changed it to −0.256 (p = 0.073), and subsequently estimating τ^2 changed it only to −0.262 (p = 0.075). Livestock adjustment, rather than τ^2 estimation or the basis change, therefore accounted for most of the attenuation (Supplementary Table S3). The alternative province-clustered period-interaction model gave positive 25 °C slopes in all three age bands, opposite in sign to all corresponding two-stage estimates. Because it used a linear year trend rather than the two-stage year spline, it was not a fully aligned specification and cannot isolate the source of this sign reversal. For ages 20–59, its 25 °C three-way slope was +0.946 log-RR per 10-percentage-point change in rural share (95% CI −1.668 to 3.560; p = 0.458), versus −2.619 (p = 0.075) in the two-stage analysis; the single-point slopes were also non-significant in the other age bands (Supplementary Table S5). The joint nine-term interaction-block test for ages 20–59 gave p = 0.074. In ages 0–19, the joint block gave $p = 1.74 \times 10^{-9}$ despite a non-significant 25 °C slope (p = 0.128); with only 11 provinces and the specification differences above, this block result is not evidence for modification at 25 °C. Joint tests address the whole cross-basis block, not the displayed single-point contrast. The earlier continuous interaction models are retained as legacy exploratory results only (Supplementary Table S2); neither single-stage design corroborates the two-stage findings.

The brucellosis economic panel provided complementary associational evidence: within-province declines in rural population share were associated with higher incidence. Sheep-stock coefficients were positive but imprecise (0.146, z = 0.69; 0.304, z = 1.45), whereas cattle-stock coefficients were positive in both displayed specifications (0.550, z = 2.39; 0.758, z = 3.47). The national mutton price, although strongly correlated with brucellosis incidence at the aggregate level (Pearson r = 0.83; Supplementary Fig. S1), had no independent association once province fixed effects and covariates were included (Table 2, Panel D). Annual mean-temperature coefficients did not show a clear association (Table 2, Panel D). This does not contradict the monthly DLNM: annual averaging removes within-year non-linear and lagged exposure variation, whereas calendar-month fixed effects in the monthly models adjust for average seasonality. The annual coefficient is therefore a different estimand, not a negative control for the monthly association. These annual-panel estimates are descriptive and are not used to identify the policy effect.

Sensitivity analyses

The policy event study did not support a causal interpretation of the plan coefficient. The joint test of pre-policy event coefficients rejected parallel pre-policy trends ($\chi^2(5) = 18.88$, p = 0.002; Supplementary Fig. S5). Although the average post-2017 association in the province- and year-fixed-effects model was an IRR of 0.264 (95% CI 0.100–0.698), year-specific post-implementation IRRs relative to 2016 ranged from 0.74 to 1.32 and were all non-significant ($p \geq 0.121$). The average coefficient therefore reflects, at least partly, differential pre-policy trajectories and is not reported as a policy effect. With livestock adjustment, rebuilding the oldest numerator as ≥65 years gave an RR at 27.8 °C of 2.03 (95% CI 1.03–4.03; 22 provinces; Supplementary Fig. S2). Adding physician density to the livestock-adjusted primary models gave RRs of 7.46 (3.62–15.41), 3.32 (2.32–4.74) and 2.87 (1.71–4.81) for ages 0–19, 20–59 and ≥60, respectively, using the same 16, 30 and 25 provinces and no fallback fits (Supplementary Table S6). Positive associations therefore remained in these revised sensitivity analyses, although the ≥65-year analysis retained the ≥60-year denominator.

Discussion

Principal findings

Across sixteen years and 604,783 notified cases, three findings stand out. First, human brucellosis in China rose substantially between 2005 and 2020, overwhelmingly through changing age-specific rates rather than population ageing. Second, the positive temperature association remained after adjustment for sheep and cattle stocks, yet

observed warming explained only 1.8–3.0% of the primary temperature-attributable burden; AF itself rose from 49–67% to 68–86% when the MRT lower search bound changed from the 5th to the 1st percentile. Third, later-period temperature associations had higher point estimates, but the common-province analysis provided limited statistical evidence that this change tracked rural depopulation ($p = 0.075$ in ages 20–59), and the alternative single-stage estimates differed in sign across all three age bands. The policy analysis further showed why before–after associations cannot be interpreted causally without examining pre-policy trends.

Comparison with previous work

Our findings extend the Chinese brucellosis literature in three directions. Descriptive studies established the post-2000s resurgence and its pastoral concentration [2]; provincial modelling linked warm, wet months to case counts but treated the climate relationship as stationary [3]. A recent nationwide analysis characterised long-term trends, seasonal patterns, persistent spatial hotspots, demographic and occupational distributions, and province-specific deviations in reported brucellosis during 2020 [5]. However, its age- and occupation-specific analyses were based on case proportions rather than population denominators, and its forecasting models did not incorporate climate or livestock covariates.

Analogous work on other climate-sensitive zoonoses has modelled hydrological and socioeconomic covariates of seasonal dynamics [6], while multi-sector European research has linked climatic, environmental, biodiversity and socioeconomic factors to hantavirus risk [4], and national analyses have documented the broad reshuffling of infectious-disease burden towards older adults [7]. Our study contributes (i) a national, age-stratified, livestock-adjusted two-stage DLNM temperature response for brucellosis; (ii) a counterfactual separation of background thermal suitability from incremental warming [8]; and (iii) a common-province temporal analysis that reports, rather than selects away, the attenuation of the rural-depopulation association.

Mechanisms and interpretation

The higher later-period point estimates are compatible with, but do not establish, a hollowing-out mechanism: as younger labour leaves pastoral production, livestock handling, slaughter and home processing may devolve onto residual workers whose exposure differs in warm months. H1 was not supported by the age pattern of the point estimates, and no corresponding rural-change association was detected in ages ≥60 ($p = 0.679$). The same-20-province decomposition showed that livestock adjustment accounted for most of the attenuation in ages 20–59, with little additional effect from estimating τ^2. The alternative province-clustered period-interaction model gave positive 25 °C slopes in all three age bands, opposite in sign to every corresponding two-stage estimate, although none of the single-point slopes was significant. Its linear year trend also differed from the two-stage year spline; the sign reversal may therefore reflect trend specification or other design differences and cannot be interpreted as evidence of modification. Together with high single-stage condition numbers, this precludes treating either single-stage specification as corroboration. The early inverse curve in ages ≥60 was also too imprecise to support a protective interpretation. The economic panel provides complementary associations for rural share; livestock-stock results were mixed, with imprecise sheep-stock coefficients and positive cattle-stock coefficients, and should not be treated as direct evidence of the proposed mechanism. Period changes in rural share, GDP per capita and health-system capacity are strongly intercorrelated ($|r| = 0.59–0.72$), so any temporal signal belongs to the broader urbanisation–development process rather than to rural share uniquely.

Strengths

The study rests on a 16-year, 31-province, single-year-age, monthly panel with 0.25° gridded climate observations. Strengths include explicit livestock adjustment with old–new curve comparison, counterfactual climatic attribution with an MRT-range sensitivity analysis, common-province period curves and meta-regression, a same-province decomposition of livestock and τ^2 contributions, and an alternative province-clustered period-interaction analysis that exposed sign differences across designs. Revised ≥65-year and physician-density sensitivities also retained

livestock adjustment. Equally important, the revision preserves discrepant results: attenuation of the rural-depopulation association, non-corroboration across single- and two-stage designs, reference-dependent AF, and violation of the policy parallel-trends assumption are reported explicitly.

Limitations

Several limitations qualify interpretation. First, all effect-modification evidence is ecological: province-level associations cannot be read as individual-level effects, and residual confounding by unmeasured province-level trends is possible. Second, the rural-depopulation result was model-dependent. In the same 20 provinces, livestock adjustment accounted for most attenuation of the 20–59-year association, whereas τ^2 contributed little; nevertheless, the alternative single-stage and two-stage estimates had opposite signs in all three age bands; the former used a linear year trend rather than the two-stage year spline and therefore was not fully aligned. The single-stage design matrices also had high condition numbers (approximately $5.2–5.7 \times 10^5$), so all interaction results remain exploratory. Third, urbanisation-related modifiers move together (intercorrelation $|r| = 0.59–0.72$), preventing clean separation of rural depopulation from income growth or health-system change. Fourth, notifiable-disease data are subject to under-reporting and diagnostic-capacity gradients; differential reporting across periods cannot be excluded. Fifth, the policy analysis failed the pre-policy parallel-trends test, so neither the average post-2017 coefficient nor the original 73–77% lower-incidence association can be interpreted as a causal policy effect. Sixth, the study window ends in December 2020; recent rural restructuring is not observable. A recent nationwide analysis identified heterogeneous province- and season-specific deviations in reported brucellosis during 2020 [5]. Although our models accounted for temporal variation and measured health-system covariates, pandemic-related changes in livestock exposure and case ascertainment during the final study year cannot be excluded. Seventh, individual livestock-contact and protective-behaviour data were unavailable, and the stronger gradient in ages 0–19, based on 16 provinces and sparse paediatric counts, should not be interpreted as individual susceptibility. Eighth, no sex- or gender-stratified analysis was possible because the harmonised province–month–age dataset contained neither variable. Ninth, the boundary-located MRT does not identify a biological minimum-risk temperature: changing the lower search bound from the 5th to the 1st percentile shifted the MRT from −8.308 to −15.649 °C, increased AF and reduced estimated warming shares, so these quantities are reference- and search-range-dependent. Finally, the ≥65-year sensitivity used a rebuilt numerator but retained the ≥60-year population denominator; it addresses age definition only, not age-specific incidence with a matched denominator.

Policy implications

Three implications follow. First, brucellosis control resources should consider older rural and pastoral residents, including age-appropriate education and protection during lambing and slaughter seasons, while recognising that individual exposure was not measured. Second, climate-health adaptation should consider population-structure change as a potential exposure modifier, but the present temporal association is not definitive enough to guide quantitative risk prediction. Third, evaluations of brucellosis programmes should use comparison groups and explicitly test pre-policy trends; our event study shows that a large average before–after association can coexist with divergent earlier trajectories and non-significant year-specific post-implementation estimates.

Conclusions

In China, temperature–brucellosis associations remained positive after livestock adjustment, whereas evidence for temporal modification by rural depopulation was limited and differed across designs. Model-estimated attributable fractions were sensitive to the MRT search range, and warming explained a small but reference-dependent share of attributable cases. Changing exposure structures require further study with individual-level exposure data and stronger quasi-experimental designs. Policy associations should be interpreted only alongside their pre-policy trajectories.

Methods

Study design and data sources

We conducted a nationwide ecological panel study at the resolution of province × calendar month × age band, covering all 31 provincial-level divisions of mainland China from January 2005 to December 2020 (192 months). The study window was locked to 2005–2020 because the data-centre release closes in 2020 (implications addressed in the Discussion). Data sources and variables are summarised in Supplementary Table S1.

Outcome data

Monthly province-level case counts by single-year or standard age group for 2005–2020 were obtained from the Public Health Science Data Center (Chinese Center for Disease Control and Prevention). Counts were harmonised into three age bands — 0–19, 20–59, and ≥60 years — chosen a priori to separate younger, working-age, and older populations. The surveillance extract did not include sex or gender variables. The final analysis panel comprised 17,856 province × month × age-band rows and 604,783 cases. Quality control comprised month-completeness checks, reconciliation against published national annual totals, and duplicate-record screening. Annual percent changes (APCs) for 2005–2020 were estimated using ordinary least-squares regressions of natural-log annual age-band-specific incidence on calendar year, with APC = $100 \times [\exp(\beta) - 1]$; 95% confidence intervals used the residual standard error of β and a normal 1.96 critical value, without joinpoints. Monthly seasonal shares were calculated within each age band.

Climate data

Daily gridded near-surface air temperature (maximum, minimum) and precipitation at 0.25° resolution were obtained from the CN05.1 dataset (1961–2020), constructed from ~2,400 Chinese meteorological stations [9,10]. Daily mean temperature was computed as the average of daily maximum and minimum. Grids were aggregated to province-months with cosine-of-latitude area weighting; the resulting series had no missing values and cross-validated against an independent station-derived series ($r = 0.996$ for temperature). Monthly mean relative humidity was obtained from NASA POWER (aggregated identically). The dataset is provided by the Arid Land Ecology and Resources Science Data Center (https://data.dcxjegi.cn).

Population denominators and covariates

Province-year populations by age band for 2005–2020 were constructed from the 2010 and 2020 censuses with intercensal interpolation and annual statistical-yearbook totals. Socioeconomic covariates (province-year) were extracted from China Statistical Yearbooks [11] and China Health Statistical Yearbooks: urbanisation rate (rural population share = 100 − urbanisation), GDP per capita, cattle and sheep stocks, hospital beds and practising physicians per 1,000 population. The annual national mutton market-fair price was extracted from the China Agricultural Product Price Survey Yearbook. The National Brucellosis Prevention and Control Plan 2016–2020 (eleven designated provinces, indicator coded from 2017) was included as a policy covariate [12].

Two-stage distributed lag non-linear models

For each age band we fitted a two-stage analysis [13]. Stage 1: within each province, a negative-binomial GLM (dispersion by profile likelihood) of monthly case counts with offset log(population/12) related cases to a cross-basis of monthly mean temperature, using a natural cubic temperature spline crossed with a 0–2-month lag dimension (one internal knot), and adjusted for precipitation (spline), relative humidity, calendar-month fixed effects, a natural cubic spline of calendar year (knots 2010, 2015), log GDP per capita, urbanisation rate, hospital

beds per 1,000, log sheep stock, log cattle stock, and the brucellosis-plan indicator. The two temperature knots (8.401 and 19.667 °C) were defined from the pooled distribution across all provinces, age bands and lagged exposures, so that province-specific coefficient vectors shared a common basis and were combinable at stage two. Provinces contributing fewer than 50 cases were excluded from pooling; a fallback specification with calendar-year fixed effects retained the livestock covariates when the full specification did not converge. The fallback was used only for Qinghai in the ≥60-year band (one province–age-band fit); all other reported first-stage fits used the full specification. Stage 2: province-specific coefficient vectors were pooled using DerSimonian–Laird random-effects multivariate meta-analysis [14]; between-province heterogeneity was quantified by Cochran's Q and I^2. Cumulative lag 0–2-month exposure–response curves are reported relative to the median temperature (14.2 °C). Original curves without livestock covariates were retained for comparison (Supplementary Fig. S4).

Climatic counterfactual attribution

Attributable components were computed following Gasparrini and Leone [8]: the minimum-risk temperature (MRT) of each pooled curve was identified within the 5th–95th percentile of observed temperatures. For each month, η was the cumulative log-RR of the observed lag 0–2 temperature history relative to the MRT, the attributable fraction was $1 - \exp(-\eta)$, and attributable cases were calculated as cases $\times [1 - \exp(-\eta)]$ and summed over months. The reported AF is therefore a model-estimated fraction of cases attributable to non-MRT temperatures, not the observed proportion of cases occurring in months warmer than the MRT. To isolate the contribution of the 2005–2020 warming trend, each province's monthly mean-temperature series was detrended using a Theil–Sen robust slope, preserving the seasonal cycle; a counterfactual lag-0–2 temperature history was reconstructed, and warming-associated excess cases were computed as observed minus counterfactual attributable cases. The warming share was calculated as 100 × (observed attributable cases − counterfactual attributable cases) / observed attributable cases. A sensitivity analysis repeated the complete attribution after reselecting the MRT within the 1st–95th percentile range, with all other specifications unchanged.

Demographic decomposition

The change in the crude national rate between 2005 and 2020 was decomposed into age-structure and age-specific-rate components using the Kitagawa method [15] with the mean of the two years' structures/rates as weights.

Socioeconomic effect modification

Between-province modification was tested by stratified pooling of the livestock-adjusted province coefficients at the median of province-mean rural population share and by weighted least-squares meta-regression of province-specific cumulative log-RRs (at 20 °C and 25 °C) on rural share. Within-province temporal modification used two equal eight-year periods, 2005–2012 and 2013–2020; the 2013 split was the midpoint of the study window and was not selected from model significance. Stage-1 models were refitted per province-period with log sheep and cattle stocks included (≥40 cases per period required). Both period-specific pooled curves and the change-on-change meta-regression were restricted to the intersection of provinces with valid estimates in both periods. The regression related per-province change in log-RR at 25 °C to change in rural population share using random-effects weighted least-squares meta-regression with residual heterogeneity estimated as τ^2; 20 °C was an alternative evaluation point. In the same 20 provinces for ages 20–59, a decomposition repeated the 25 °C regression with and without livestock adjustment and with fixed-effect versus random-τ^2 weighting; the legacy age-band basis was also compared with the current common basis. An alternative single-stage period-interaction sensitivity model used the same common provinces, periods, 25 °C contrast and Δrural coding, but retained a linear year trend rather than the two-stage year spline. It included temperature cross-basis, period, Δrural and their full interactions, province and calendar-month fixed effects, livestock, precipitation, humidity, linear year and policy covariates. Province-clustered CR1 standard errors were used; the 25 °C three-way slope per 10-percentage-point change used t inference with provinces − 1 degrees of freedom, and the nine-term interaction block used a rank-aware F test. A legacy continuous province-

centred interaction model with model-based standard errors was retained only as a supplementary comparison because its estimand and province composition differed.

Exploratory livestock-density modification

Province-mean sheep and cattle stocks per 100 rural residents were calculated from annual stocks and rural population. Reusing the livestock-adjusted province-specific DLNM coefficients, random-effects meta-regression related cumulative log-RR at 25 °C versus each age band's median temperature to log2 livestock density; estimates are expressed per doubling. Six primary age-band × species tests were adjusted using the Benjamini–Hochberg false-discovery-rate procedure. Sensitivity analyses added rural share and log GDP per capita, baseline mean temperature, and mutual livestock adjustment; used total-population and absolute-stock denominators; compared precision-weighted and unweighted HC3 estimators; and examined leave-one-province-out influence. Descriptive median-split pooled RRs were also calculated. No first-stage model was refitted. Detailed adjustment, weighting, influence, descriptive, secondary-contrast and correlation analyses are reported in Supplementary Tables S8–S13. These analyses were defined as exploratory and are not independent causal estimates of livestock effects.

Brucellosis economic-driver panel

An annual province fixed-effects negative-binomial panel (31 provinces × 16 years = 496 province-years) estimated the joint associations of brucellosis incidence with log sheep stock, log cattle stock, rural population share, log GDP per capita, hospital beds per 1,000 population, annual mean temperature, annual precipitation, and the national plan indicator. Spec A additionally adjusted for secular time using a natural cubic spline of calendar year; Spec B replaced that spline with the national log mutton price. Because the eleven plan provinces were selected on burden, we further fitted an event-study model with province and calendar-year fixed effects, the same covariates, and province-clustered standard errors. Event time was relative to implementation in 2017, with 2016 as reference and 2005–2011 binned as ≤2011. The joint Wald test covered the five pre-policy event coefficients. A separate province- and year-fixed-effects model estimated the average post-2017 association descriptively.

Sensitivity analyses

Sensitivity analyses comprised (i) rebuilding the oldest age-band numerator as ≥65 years from single-year-age raw records, (ii) adding practising physicians per 1,000 to the livestock-adjusted models using the same provinces as the corresponding primary analyses, (iii) comparing curves before and after livestock adjustment, (iv) restricting period analyses to common provinces and decomposing livestock and τ^2 contributions, (v) the alternative province-clustered period-interaction model, (vi) the legacy continuous interaction model, (vii) the 1st-percentile MRT search, and (viii) the policy event study. The ≥65-year sensitivity retained the available ≥60-year population denominator and therefore did not constitute a fully re-denominated ≥65-year incidence analysis. Analyses used Python 3.11 (statsmodels, patsy); two-sided $\alpha = 0.05$. The study is ecological; no individual-level causal inference is drawn.

Use of generative AI in manuscript preparation

During the preparation of this work the authors used Kimi (Moonshot AI) for language editing, structural revision, and reference-format checking. After using this tool, the authors reviewed and edited the content as needed and take full responsibility for the content of the published article.

Data availability

The surveillance case data were obtained from the Public Health Science Data Center (Chinese Center for Disease Control and Prevention) under a data-use agreement. They are not publicly available because of the conditions of that agreement, but are accessible from the Center upon reasonable request and with its permission. Derived province–month analysis data contain these restricted surveillance counts and therefore cannot be publicly deposited. CN05.1 climate data are available from the Arid Land Ecology and Resources Science Data Center (https://data.dcxjegi.cn), and humidity data are publicly available from NASA POWER (https://power.larc.nasa.gov). Population and socioeconomic data are from published censuses and yearbooks cited in the article.

Code availability

The custom Python 3.11 analysis code is available from the corresponding author on reasonable request and will be made available to editors and reviewers upon request.

References

1. Laine, C. G., Johnson, V. E., Scott, H. M. & Arenas-Gamboa, A. M. Global estimate of human brucellosis incidence. *Emerg. Infect. Dis.* **29**, 1789–1797 (2023). https://doi.org/10.3201/eid2909.230052

2. Lai, S. et al. Changing epidemiology of human brucellosis, China, 1955–2014. *Emerg. Infect. Dis.* **23**, 184–194 (2017). https://doi.org/10.3201/eid2302.151710

3. Huang, S. et al. Risk effects of meteorological factors on human brucellosis in Jilin province, China, 2005–2019. *Heliyon* **10**, e29611 (2024). https://doi.org/10.1016/j.heliyon.2024.e29611

4. Guo, J. et al. A pan-European assessment of multi-sector drivers of human hantavirus risk: climate, biodiversity, and socio-economic factors as key determinants. *Environ. Res.* **298**, 124282 (2026). https://doi.org/10.1016/j.envres.2026.124282

5. Xu, M. et al. A multi-model counterfactual analysis of human brucellosis in China: spatiotemporal epidemiology and heterogeneous pandemic-associated deviations in 2020. *Int. J. Infect. Dis.* **172**, 109119 (2026). https://doi.org/10.1016/j.ijid.2026.109119

6. Ge, H. H. et al. Combined effects of hydrological conditions and socioeconomic factors on the seasonal dynamics of severe fever with thrombocytopenia syndrome in China, 2011–2022: a modelling study. *Lancet Reg. Health West. Pac.* **58**, 101564 (2025). https://doi.org/10.1016/j.lanwpc.2025.101564

7. Lin, S. H. et al. Epidemiological analysis of infectious diseases in older people in China from 2014 to 2022: a population-based study. *Lancet Reg. Health West. Pac.* **64**, 101729 (2025). https://doi.org/10.1016/j.lanwpc.2025.101729

8. Gasparrini, A. & Leone, M. Attributable risk from distributed lag models. *BMC Med. Res. Methodol.* **14**, 55 (2014). https://doi.org/10.1186/1471-2288-14-55

9. Wu, J. & Gao, X. J. A gridded daily observation dataset over China region and comparison with the other datasets. *Chin. J. Geophys.* **56**, 1102–1111 (2013). https://doi.org/10.6038/cjg20130406

10. Xu, Y. et al. A daily temperature dataset over China and its application in validating a RCM simulation. *Adv. Atmos. Sci.* **26**, 763–772 (2009). https://doi.org/10.1007/s00376-009-9029-z

11. National Bureau of Statistics of China. China Statistical Yearbook (annual editions 2006–2021). *China Statistics Press* , Beijing (2006–2021).

12. Ministry of Agriculture and National Health and Family Planning Commission of the People's Republic of China. National Brucellosis Prevention and Control Plan (2016–2020). Beijing (2016). http://www.moa.gov.cn/govpublic/SYJ/201609/t20160909_5270524.htm (accessed 30 October 2026) [in Chinese].

13. Gasparrini, A., Armstrong, B. & Kenward, M. G. Distributed lag non-linear models. *Stat. Med.* **29**, 2224–2234 (2010). https://doi.org/10.1002/sim.3940

14. DerSimonian, R. & Laird, N. Meta-analysis in clinical trials. *Control. Clin. Trials* **7**, 177–188 (1986). https://doi.org/10.1016/0197-2456(86)90046-2

15. Kitagawa, E. M. Components of a difference between two rates. *J. Am. Stat. Assoc.* **50**, 1168–1194 (1955). https://doi.org/10.1080/01621459.1955.10501299

Acknowledgements

We thank the Data-center of China Public Health Science and the Arid Land Ecology and Resources Science Data Center for data access.

Funding

This work was supported by the Natural Science Basic Research Program Youth Project of the Shaanxi Provincial Science and Technology Department [2023-JC-QN-0830]. The funder had no role in study design; data collection, analysis, or interpretation; manuscript writing; or the decision to submit the article for publication.

Author contributions

F.W.: Conceptualization, Data curation, Formal analysis, Investigation, Methodology, Software, Writing – original draft. Y.H.: Conceptualization, Data curation, Investigation, Methodology, Validation, Writing – original draft, Writing – review & editing. Y.D.: Investigation, Validation. M.K.: Data curation, Validation. Y.L.: Data curation, Investigation, Methodology, Validation. T.C.: Supervision, Writing – review & editing. Z.T.: Conceptualization, Funding acquisition, Supervision, Writing – review & editing. All authors read and approved the final manuscript.

Competing interests

The authors declare no competing interests.

Ethics declarations

Ethics approval and consent to participate

This nationwide ecological study used only anonymised, aggregated surveillance counts and publicly available statistics; no identifiable individual-level data were accessed. All procedures complied with relevant institutional

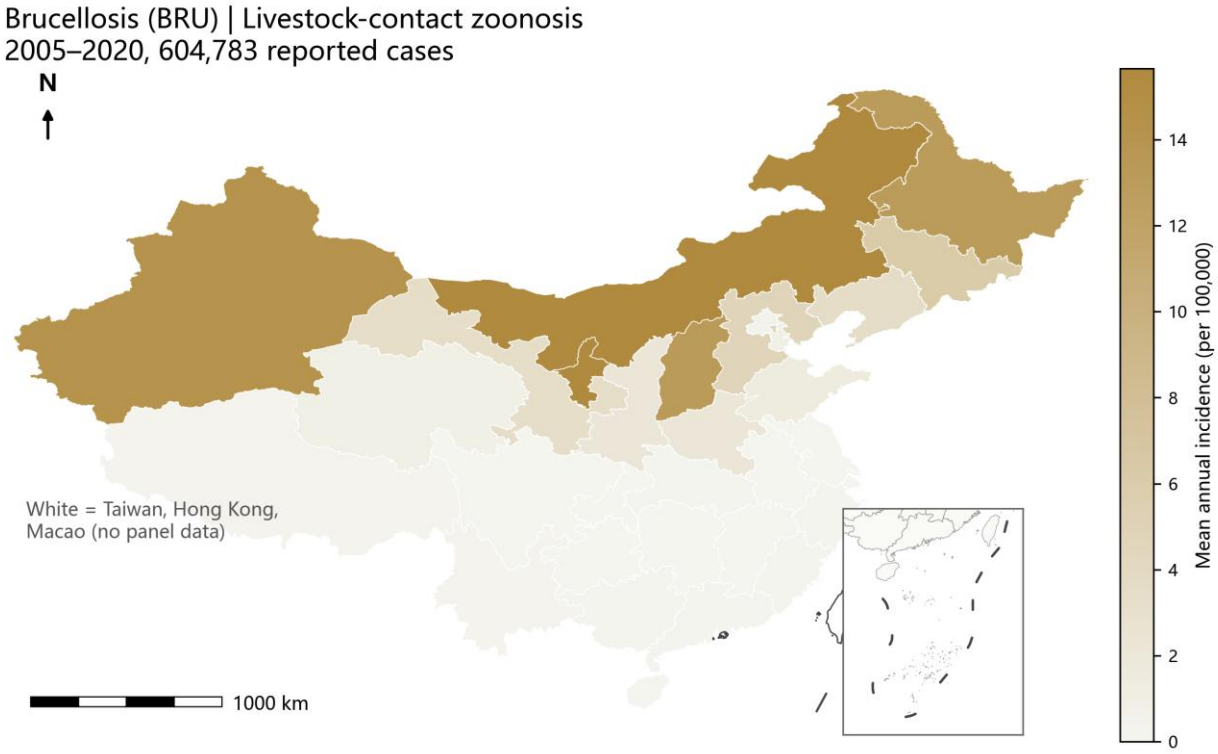
and national regulations. Institutional review board approval and informed consent were not required for these secondary, aggregated data.

Consent for publication

Not applicable.

Figure legends

Fig. 1. Provincial mean annual brucellosis incidence, 2005–2020.



Note: boundaries follow national base geographic information data, including Taiwan Province, the South China Sea islands and the dashed line; Taiwan, Hong Kong and Macao are not covered by the surveillance panel and are shown in white.

The choropleth shows Taiwan, Hong Kong and Macao in white because they were not in the surveillance panel; South China Sea islands and boundary are shown in the inset. Map lines delineate study areas and do not necessarily depict accepted national boundaries.

Fig. 2. Proportion of brucellosis cases aged ≥60 years, 2005–2020.

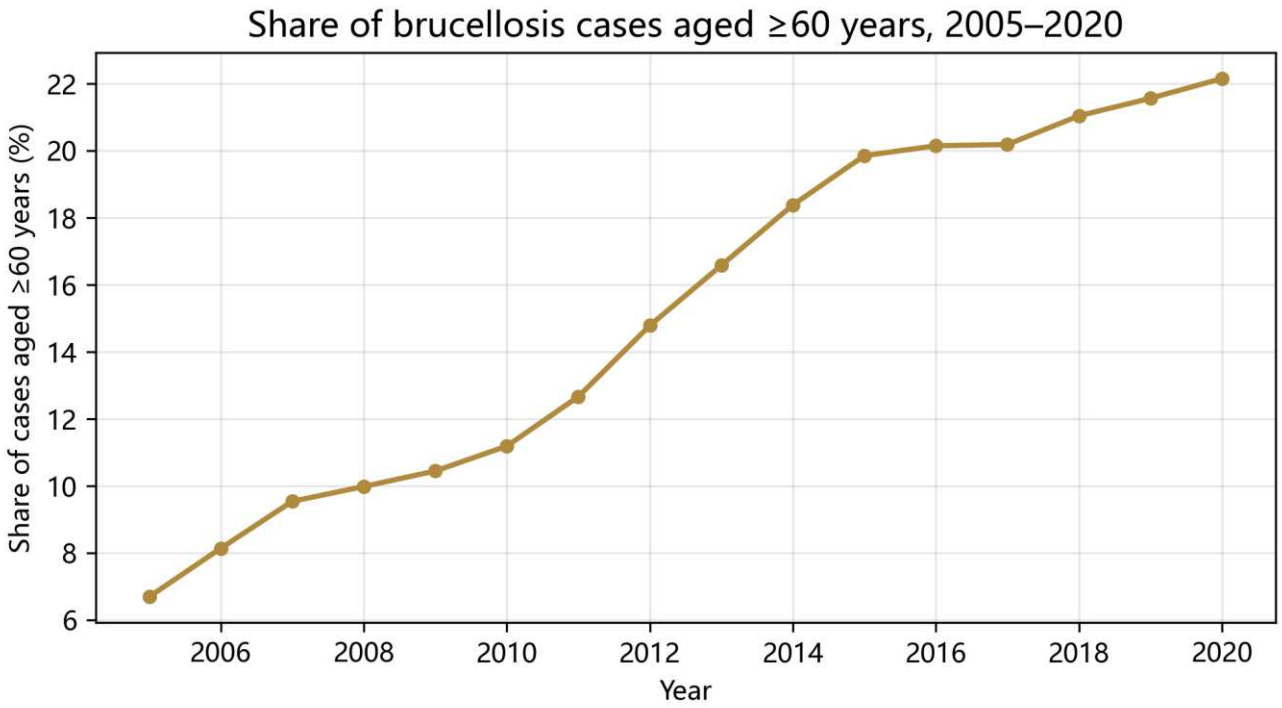
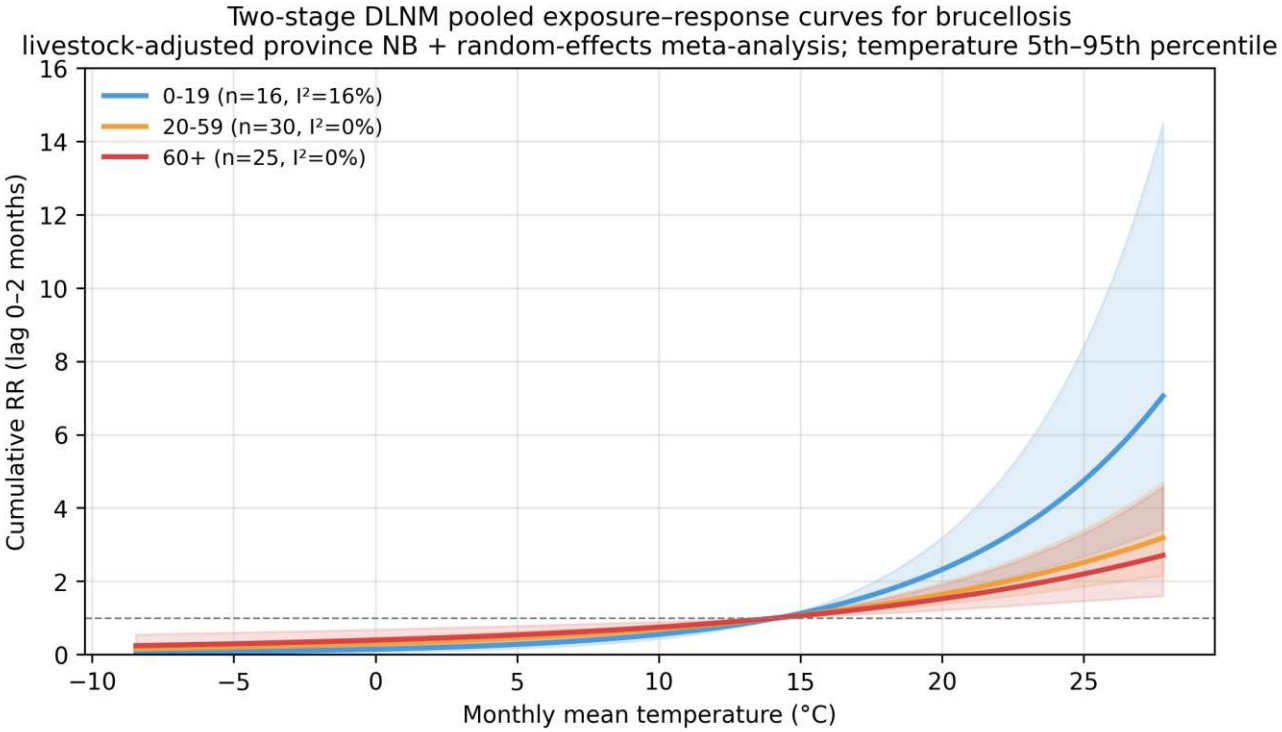
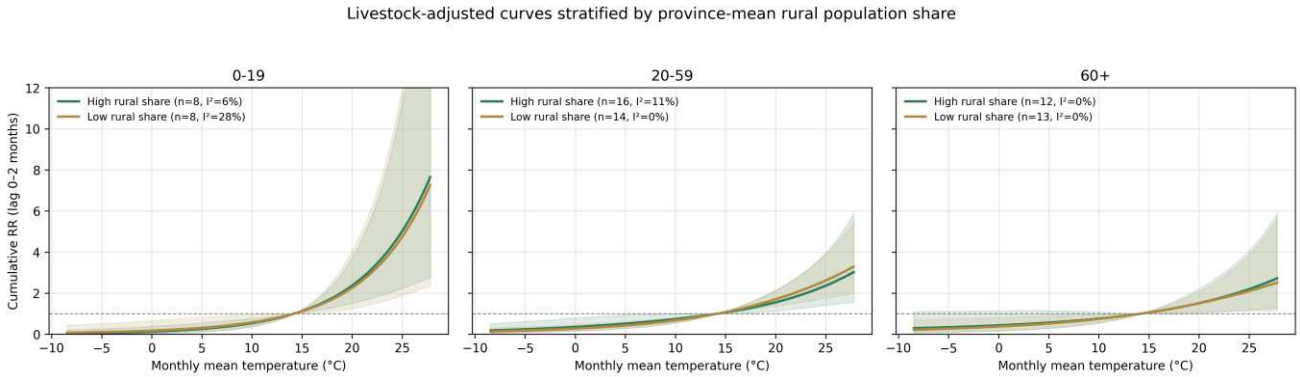


Fig. 3. Livestock-adjusted two-stage distributed lag non-linear model pooled cumulative temperature–morbidity relative-risk curves by age band.



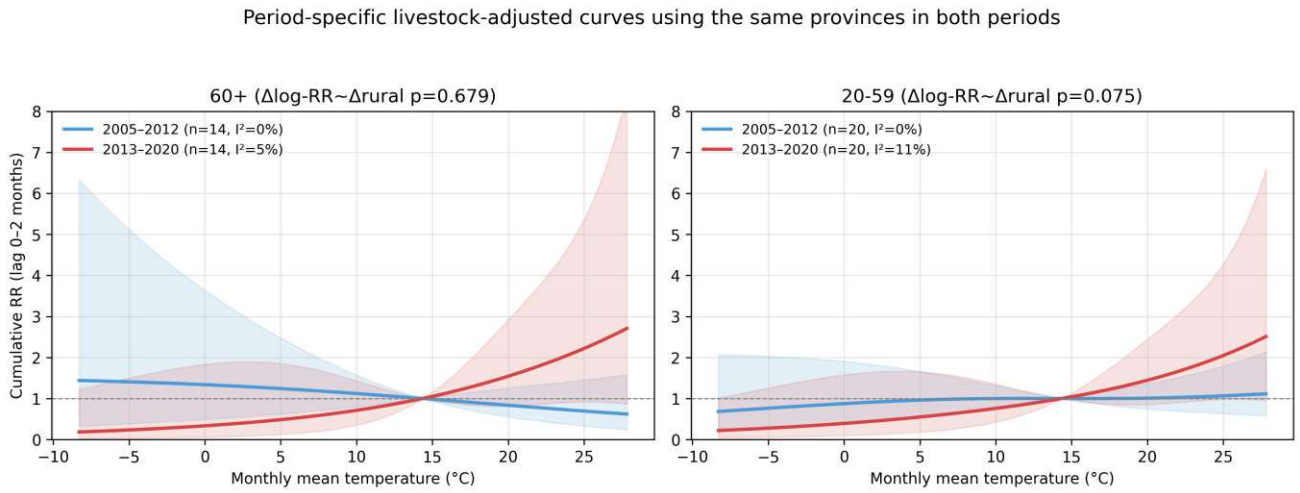
Estimates are cumulative over lag 0–2 months relative to the median temperature (14.2 °C). Shading represents 95% confidence intervals.

Fig. 4. Livestock-adjusted pooled temperature–incidence curves stratified by province-mean rural population share.



Curves use a median split and are cumulative over lag 0–2 months relative to median temperature. Shading represents 95% confidence intervals.

Fig. 5. Period-specific livestock-adjusted pooled curves, 2005–2012 versus 2013–2020.



Analyses use the same provinces in both periods; p values are from change-on-change meta-regression. Shading represents 95% confidence intervals.

Tables

Table 1. Brucellosis burden and risk-reshuffling overview, 2005–2020

Cases	Mean annual rate /100,000	Peak year (rate)	Top-3 provincial-level divisions (rate /100,000)	≥60 share 2005→2020	APC ≥60 band, %/yr (95% CI)	Peak-3-month concentration
604,783	2.800	2014 (4.201)	Inner Mongolia (45.4), Ningxia (17.1), Xinjiang (14.2)	6.7%→22.2%	+10.8 (7.3 to 14.5)	38.3% (Apr–Jun; peak May)

Table 2. Driver summary: climatic attribution, demographic decomposition, effect modification, and economic panel

Panel A. Climatic counterfactual attribution (2005–2020; reference = minimum-risk temperature)

Age band	Case coverage, % (n)	Attributable fraction to non-MRT temperature, %	Warming-associated excess cases	Warming share of attributable cases, %	MRT, °C
0–19	97.6% (24,779)	67.0	+302	1.8	−8.3
20–59	99.5% (477,176)	48.9	+7,100	3.0	−8.3
≥60	99.5% (99,448)	51.5	+1,369	2.7	−8.3

Panel B. Kitagawa decomposition of crude-rate change, 2005→2020 (per 100,000)

Rate 2005	Rate 2020	Δ	Age-structure component	Age-specific-rate component
1.432	3.351	+1.919	+0.069	+1.850

Panel C. Effect modification: change-on-change meta-regression (Δlog-RR at 25 °C ~ Δ rural population share; split 2013)

Age band	Provinces	Slope per pp Δrural	p
≥60	14	−0.091	0.679
20–59	20	−0.262	0.075

Panel D. Economic panel (province fixed-effects negative-binomial models; coefficients and z statistics)

Variable	Spec A (year spline)	Spec B (mutton price)
lprice	—	−0.150 (z = −0.49)
lsheep	+0.146 (z = 0.69)	+0.304 (z = 1.45)
lcattle	+0.550 (z = 2.39)	+0.758 (z = 3.47)
rural	−0.099 (z = −3.62)	−0.100 (z = −3.75)
lgdp	+1.171 (z = 2.51)	+1.147 (z = 2.84)
beds_per1k	+0.162 (z = 1.34)	+0.217 (z = 1.92)
tmean	−0.004 (z = −0.04)	+0.134 (z = 1.35)
pre	+0.0001 (z = 1.49)	+0.0003 (z = 2.88)
pol (National Plan)	−1.308 (z = −6.35)	−1.471 (z = −7.82)

Notes: APC, annual percent change; CI, confidence interval; DLNM, distributed lag non-linear model; MRT, minimum-risk temperature; pp, percentage point. In Panel A, AF is the model-estimated attributable fraction from the livestock-adjusted pooled curves, not the observed percentage of cases in months above the MRT. Case coverage uses cases with complete lag-2 exposure in eligible provinces. Across the three age bands, 2,546 cases lacked complete lag-2 exposure and 834 cases were in provinces excluded by case thresholds or model convergence, accounting for the 3,380-case difference between the full panel (604,783) and covered cases (601,403). Panel C uses the same provinces in both periods. In Panel D, lprice denotes log national mutton price; lsheep and lcattle, log sheep and cattle stocks; rural, rural population share; lgdp, log GDP per capita; beds_per1k, hospital beds per 1,000 population; tmean, annual mean temperature; pre, annual precipitation; and pol, the National Brucellosis Plan indicator. Panel D coefficients are descriptive; the policy event study rejected parallel pre-policy trends and precludes causal interpretation of pol.

Supplementary Files

This is a list of supplementary files associated with this preprint. Click to download.

- SupplementaryInformationBRUScientificReports20261030.pdf